

See discussions, stats, and author profiles for this publication at: <https://www.researchgate.net/publication/230795811>

Theoretical Study of Atomic Oxygen on Gold Surface by Huckel Theory and DFT Calculations

ARTICLE *in* THE JOURNAL OF PHYSICAL CHEMISTRY A · SEPTEMBER 2012

Impact Factor: 2.69 · DOI: 10.1021/jp306906j · Source: PubMed

CITATIONS

11

READS

64

4 AUTHORS, INCLUDING:



[Keju Sun](#)

National Institute of Advanced Industrial Scie...

28 PUBLICATIONS 488 CITATIONS

SEE PROFILE



[Masanori Kohyama](#)

National Institute of Advanced Industrial Scie...

152 PUBLICATIONS 1,533 CITATIONS

SEE PROFILE

Theoretical Study of Atomic Oxygen on Gold Surface by Hückel Theory and DFT Calculations

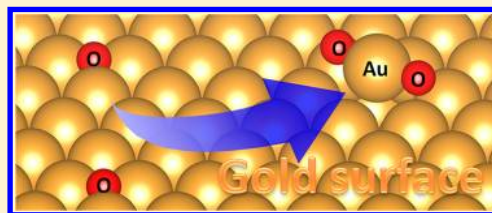
Keju Sun,^{*,†,‡} Masanori Kohyama,[†] Shingo Tanaka,[†] and Seiji Takeda[‡]

[†]Research Institute for Ubiquitous Energy Devices, National Institute of Advanced Industrial Science and Technology (AIST), 1-8-31 Midorigaoka, Ikeda, Osaka 563-8577, Japan

[‡]The Institute of Scientific and Industrial Research, Osaka University, 8-1 Mihogaoka, Ibaraki, Osaka 567-0047, Japan

S Supporting Information

ABSTRACT: It is fundamental to understand the behavior of atomic oxygen on gold surfaces so as to elucidate the mechanism of nano gold catalysts for low-temperature CO oxidation reactions since the atomic oxygen on gold system is an important intermediate involved in both the processes of O₂ dissociation and CO oxidation. We performed theoretical analysis of atomic oxygen adsorption on gold by using Hückel theory. It is found that formation of linear O–Au–O structure on Au surfaces greatly stabilizes the atomic oxygen adsorption due to stronger bond energy and bond order, which is confirmed subsequently by density functional theory (DFT) calculations. The linear O–Au–O structure may explain the surprising first order kinetics behavior of O₂ desorption from gold surfaces. This view of the linear O–Au–O structure as the natural adsorption status is quite different from the conventional view, which may lead to new understanding toward the reaction mechanism of low-temperature CO oxidation reaction on nano gold catalysts.



■ INTRODUCTION

In recent years, nano gold catalysts have been widely studied due to a large amount of new potential applications in the chemical industry such as oxidations^{1–4} or selective oxidations.^{5–7} Extensive studies have been performed to analyze the origin of such high catalytic activity and selectivity, from both the theoretical and experimental points of view,^{2,3,8–16} while many questions remain concerning even the relatively simple and widely studied reaction of CO oxidation. One barrier to understand the CO oxidation on the Au surface is to find out the nature of adsorbed atomic oxygen on the Au surface because it is an important intermediate involved in both the processes of O₂ dissociation and CO oxidation.

Despite numerous studies, it remains many puzzles about the nature of the adsorbed atomic oxygen on gold surfaces in both theoretical and experimental fields. For instance, using density functional theory (DFT) calculations, Fajin et al.^{17,18} have studied in detail oxygen atom adsorption in the stepped Au (321) surface and found that oxygen atoms prefer the interaction with surface cavities on step surfaces, while Liu et al.¹⁹ demonstrated that the most stable site for atomic oxygen on Au step surfaces is the bridge site of a step edge. So what is the most stable structure of the atomic oxygen adsorption on Au surfaces? Experimentally, Parker et al.²⁰ studied the interaction of chemisorbed oxygen with the Au(111) surface by temperature programmed desorption (TPD) and found that the desorption curves are well described by first order kinetics, which is unexpected for the combination of atomically adsorbed oxygen species. The surprising first order kinetics of O₂ desorption from the Au surface was observed on different gold single crystal surfaces.^{2,21–23} The unusual desorption

behavior was considered to be important in determining the reactivity of oxygen on the Au surface,²² while the nature of the adsorbed oxygen species and the reason of the unusual kinetics are still unclear.

In this work, the interaction between atomic oxygen and gold was first investigated by Hückel theory,^{24,25} and then, the results were examined by DFT calculations. The behaviors of oxygen atoms on Au surfaces involving the geometries and adsorption energies at different situations and the reason of the unusual desorption kinetics were analyzed. Although Hückel theory is not a quantitative theory, it can grasp the essence and tendency of chemical phenomena and hence provide some interesting and valuable predictions. At the same time, the DFT calculation is a powerful tool to deal with various systems with enough accuracy comparable to experimental data, while it is not necessarily good at predictions in the tendency of chemical phenomena, due to the nature of the DFT theory relying only on the electron density as well as numerical complexities. The present study shows the power of complementary combination between Hückel theory and DFT calculations to understand the atomic oxygen adsorption on various gold systems, as our previous experience of CO adsorption on various gold systems.²⁶

■ METHOD OF DFT CALCULATIONS

To examine the validity of the predictions by Hückel theory, DFT calculations using Vienna Ab Initio Simulation Package

Received: July 12, 2012

Revised: August 31, 2012

Published: September 4, 2012

(VASP)²⁷ were applied to the systems of oxygen adsorption on gold. The exchange-correlation energy and potential are described by generalized gradient approximation in the form of PBE.²⁸ The calculated lattice constant for bulk Au was 4.17 Å, which is in reasonable agreement with the experimental value of 4.08 Å and the previous theoretical value of 4.18 Å.⁴ Plane waves are used to expand wave functions with a cutoff of 400 eV for projector augmented wave (PAW) potentials.^{29,30} The criteria for the convergence in the structural determination was the residual force less than 0.02 eV Å⁻¹. All Au surfaces are modeled by a five-layered slab with a vacuum thickness of 15 Å, where the adsorbed species are placed on one side. The top three layers are relaxed, while the two bottommost layers are fixed at their bulk structure. A 3 × 3 supercell is used for the Au(111), Au(100), and Au(110) surfaces with the Monkhorst–Pack (MP) 4 × 4 × 1 *k*-point mesh. A 1 × 4 supercell is used for the Au(211) surface with the MP 4 × 3 × 1 *k*-point mesh. A 2 × 2 supercell is used for the Au(321) surface with the MP 3 × 3 × 1 *k*-point mesh. The oxygen atom adsorption energies for the most stable sites were computed with denser meshes (9 × 9 × 1 for Au(111), Au(100), and Au(110) surfaces, 8 × 5 × 1 for Au(211) surface, 6 × 6 × 1 for Au(321) surface), and the energy differences were found less than 0.05 eV. For Au–O cluster models, a supercell of 18 × 19 × 20 Å³ is used with the MP 1 × 1 × 1 mesh. The reaction barrier is calculated by force reversed method.³¹ The atomic oxygen adsorption energy is defined as $E_{\text{ads}} = E(\text{surface} + \text{O}) - E(\text{surface}) - E(\text{O})$, where $E(\text{surface} + \text{O})$ corresponds to the energy of a gold surface with oxygen adsorption, $E(\text{surface})$ is the energy of a clean relaxed gold surface, and the $E(\text{O})$ is the energy of an isolated O atom. Spin polarization is considered during all the calculations.

PREDICTION BY HÜCKEL THEORY

In the system consisting of only atomic oxygen and gold, it is possible to consider five different constitutional units between Au and O, namely, Au–O, Au–O–Au, O–Au–O, O–(Au)_{*n*}, and Au–(O)_{*n*} (*n* ≥ 3) units. Various structures of adsorbed atomic oxygen on Au surfaces are regarded to be constructed by these units or their combinations. The analysis of the O–Au bond strength in these units by Hückel theory will help us to understand the interaction between O and Au. Similarly to the analysis of CO adsorption on a Au surface,²⁶ the interaction between gold and oxygen is also separated into two parts: one is the σ -bonding contribution and the other is the π -bonding contribution.

According to molecular orbital theory, the closeness of the atomic orbital levels of oxygen and gold is required to form stable Au–O molecular orbitals. The 5d orbitals of gold instead of 6s orbitals are considered to be combined with the 2p orbitals of oxygen since the 5d orbital levels of gold are more close to 2p orbital levels of oxygen. There are five 5d atomic orbitals for Au atom and three 2p atomic orbitals for O atom, and they can form three bonds of Au–O (one σ -bond and two π -bonds). Only three of five 5d orbitals of Au atoms can participate in the bond formation, and the remaining two 5d orbitals form the nonbonding orbitals. For example, if the *z* direction is the direction of the Au–O axis, *d*_{z²} orbital of Au and *p*_{*z*} orbital of O form the σ -bond and *d*_{xz}/*d*_{yz} orbitals of Au and *p*_{*x*}/*p*_{*y*} orbitals of O form the two π -bonds. The remaining *d*_{x²–y²} and *d*_{xy} orbitals do not participate in the Au–O bond formation. Therefore, only one 5d atomic orbital is involved in every one Au–O bond. For gold, there are 10 electrons in five 5d orbitals (two electrons in each 5d orbital). As a result, to

form every bond of Au–O involving one σ -bond and two π -bonds, the contributive electron number from 5d orbitals of gold is always two. For oxygen, there are a total of four electrons on three 2p orbitals, and so there are one, one, and two electrons on the three 2p orbitals, respectively. In this work, two electrons from an oxygen atom is assigned to the σ -bond, and the remaining two electrons are assigned to two π -bonds; the electron distributions in Au–O, Au–O–Au, and O–Au–O molecular orbitals are shown in Figure 1.

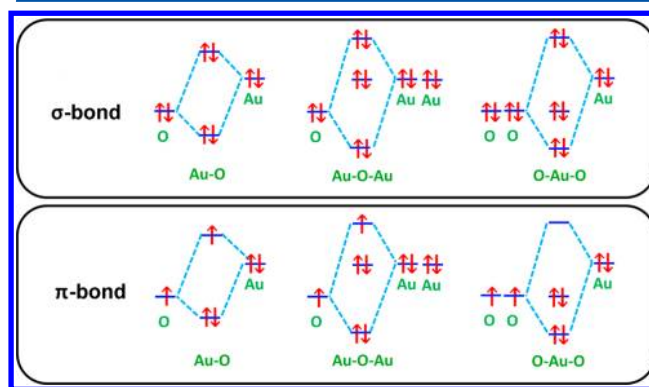


Figure 1. Schematic diagrams for the electron distributions in Au–O, Au–O–Au, and O–Au–O molecular orbitals. The other π -bond is omitted due to reiteration.

Here, more electrons are received from oxygen for the σ -bond than the π -bond because the electrons prefer to occupy the σ -antibonding orbital rather than occupy the π -antibonding orbital. The origin is that there are some constructive interactions in σ -antibonding orbital. Figure 2 shows the formation of antibonding orbitals of Au–O in σ -bond and π -bond. The *p* orbital of oxygen consists of two parts with opposite phase signs, as denoted as + ψ and – ψ . The place where the phase signs change is a nodal plane. There is one nodal plane for every *p* orbital, and there are two nodal planes for every *d* orbital. For the σ -antibonding orbital, it is found that the space between Au and O is separated to two parts. One part is the region of + ψ – ψ , where the atomic orbitals from oxygen and gold are out of phase, thereby the interaction in this region is destructive, which should contribute to the rise of the energy level of the σ -antibonding orbital of Au–O. The other part is the region of + ψ + ψ , where the atomic orbitals from oxygen and gold are in phase; therefore, the interaction in this region is constructive (like bonding orbital component), contributing to the lowering of the energy level for the σ -antibonding orbital of Au–O. However, for the π -antibonding orbital, the whole region between Au and O is only the region of + ψ – ψ . Thus, the π -antibonding orbital of Au–O is totally destructive, which should contribute to the strong rise of the energy level for the π -antibonding orbital of Au–O. Therefore, it is expected that the energy level of the π -antibonding orbital is higher than that of the σ -antibonding orbital, which can be also proved by DFT calculations.

From Figure 1, it is found that all the orbitals in σ -bond are filled for Au–O, Au–O–Au, and O–Au–O molecules. Similarly, all the orbitals in σ -bond are also filled for Au–(O)_{*n*} and O–(Au)_{*n*} molecules. Therefore, the contribution of σ -bond could be ignored, and the dominant contribution should be assigned to the contribution of π -bond. Thus, we only focus on the contribution of the π -bond in the following,

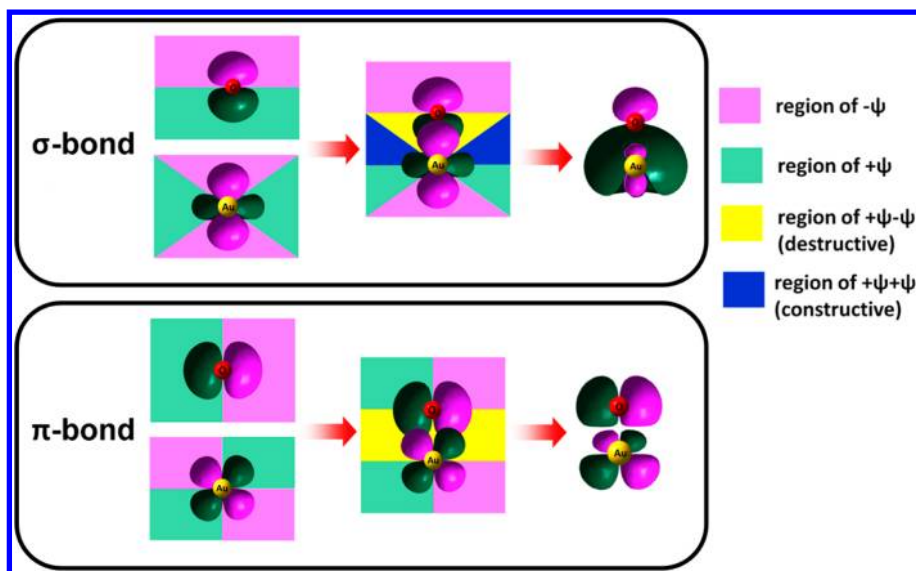


Figure 2. Formation of antibonding orbitals of Au–O in σ -bond and π -bond. The other π -bond is omitted due to reiteration.

and only one π -bond is discussed since the two π -bonds are identical. For the π -bonding contribution, the basic secular determinant for the Au–O molecule is given as

$$\begin{vmatrix} \alpha_{\text{O}} - E & \beta_{\text{O-Au}} \\ \beta_{\text{O-Au}} & \alpha_{\text{Au}} - E \end{vmatrix} = 0 \quad (1)$$

The parameters of α_{O} and α_{Au} are the values of relevant Coulomb integrals for O and Au atoms, namely, the energy levels of O and Au orbitals (p_x or p_y for O and d_{xz} or d_{yz} for Au). The parameter of $\beta_{\text{O-Au}}$ represents the interaction between the O and Au orbitals. If we assume the relations as $\alpha_{\text{Au}} = \alpha$, $\beta_{\text{O-Au}} = \beta$, and $\alpha_{\text{O}} = \alpha + h\beta$, the solutions of the secular determinant for Au–O are given by

$$\begin{cases} E_1^{\text{O-Au}} = \alpha - \frac{-h - \sqrt{h^2 + 4}}{2}\beta \\ E_2^{\text{O-Au}} = \alpha - \frac{-h + \sqrt{h^2 + 4}}{2}\beta \end{cases} \quad (2)$$

Since the energy level of 5d orbitals of Au is higher than 2p orbitals of O, α_{O} is lower than α_{Au} and h is a positive value. Furthermore, since β is negative, $E_1^{\text{O-Au}}$ is the energy of a bonding orbital, and $E_2^{\text{O-Au}}$ is the energy of an antibonding orbital. For every π -bond, one electron comes from an O atom and two electrons come from an Au atom, and they form a filled bonding orbital and a half-filled antibonding orbital as shown in Figure 1. Therefore, the contribution of every π -bond to the bond of Au–O is

$$\begin{aligned} \Delta E_{\pi}^{\text{O-Au}} &= 2E_1^{\text{O-Au}} + E_2^{\text{O-Au}} - 2\alpha_{\text{Au}} - \alpha_{\text{O}} \\ &= \frac{h + \sqrt{h^2 + 4}}{2}\beta \end{aligned} \quad (3)$$

Similar to Au–O, the contributions of every π -bond to the bonds of Au–O–Au and O–Au–O are obtained by

$$\begin{aligned} \Delta E_{\pi}^{\text{Au-O-Au}} &= 2E_1^{\text{Au-O-Au}} + 2E_2^{\text{Au-O-Au}} + E_3^{\text{Au-O-Au}} \\ &\quad - 4\alpha_{\text{Au}} - \alpha_{\text{O}} \\ &= \frac{h + \sqrt{h^2 + 8}}{2}\beta \end{aligned} \quad (4)$$

$$\begin{aligned} \Delta E_{\pi}^{\text{O-Au-O}} &= 2E_1^{\text{O-Au-O}} + 2E_2^{\text{O-Au-O}} - 2\alpha_{\text{Au}} - 2\alpha_{\text{O}} \\ &= \left(h + \sqrt{h^2 + 8}\right)\beta \end{aligned} \quad (5)$$

It is convenient to extend to the π -bond of $\text{O}-(\text{Au})_n$ and $\text{Au}-(\text{O})_n$ ($n \geq 3$) models

$$\begin{aligned} \Delta E_{\pi}^{\text{O}-(\text{Au})_n} &= 2E_1^{\text{O}-(\text{Au})_n} + 2E_2^{\text{O}-(\text{Au})_n} + \dots + E_{n+1}^{\text{O}-(\text{Au})_n} \\ &\quad - 2n\alpha_{\text{Au}} - \alpha_{\text{O}} \\ &= \frac{h + \sqrt{h^2 + 4n}}{2}\beta \end{aligned} \quad (6)$$

$$\begin{aligned} \Delta E_{\pi}^{\text{Au}-(\text{O})_n} &= 2E_1^{\text{Au}-(\text{O})_n} + 2E_2^{\text{Au}-(\text{O})_n} + \dots - 2\alpha_{\text{Au}} - n\alpha_{\text{O}} \\ &= \left(h + \sqrt{h^2 + 4n}\right)\beta \end{aligned} \quad (7)$$

Equations 6 and 7 show that the contribution of the π -bond of $\text{O}-(\text{Au})_n$ (or $\text{Au}-(\text{O})_n$) will raise as the increase of the coordinate number for O (or Au). This indicates that the O (or Au) prefers to connect with more Au (or O) atoms, thereby we can predict that the oxygen atom prefers to adsorb at multifold sites (hole sites) rather than at the top site of Au surfaces. However, because of the limitation of space, the coordinate number for Au could not increase unlimitedly. Instead, it has to face a severe competition from Au–Au bonds. Therefore, the efficiency of every Au–O bond is more important. If we divide the contribution of π -bond into every Au–O bond, we can obtain

$$\Delta \varepsilon_{\pi}^{\text{O-Au}} = \frac{\Delta E_{\pi}^{\text{O-Au}}}{1} = \frac{h + \sqrt{h^2 + 4}}{2}\beta \quad (8)$$

$$\Delta \varepsilon_{\pi}^{\text{Au-O-Au}} = \frac{\Delta E_{\pi}^{\text{Au-O-Au}}}{2} = \frac{h + \sqrt{h^2 + 8}}{4}\beta \quad (9)$$

$$\Delta\epsilon_{\pi}^{\text{O-Au-O}} = \frac{\Delta E_{\pi}^{\text{O-Au-O}}}{2} = \frac{h + \sqrt{h^2 + 8}}{2}\beta \quad (10)$$

$$\Delta\epsilon_{\pi}^{\text{O-(Au)}_n} = \frac{\Delta E_{\pi}^{\text{O-(Au)}_n}}{n} = \frac{h + \sqrt{h^2 + 4n}}{2n}\beta \quad (11)$$

$$\Delta\epsilon_{\pi}^{\text{Au-(O)}_n} = \frac{\Delta E_{\pi}^{\text{Au-(O)}_n}}{n} = \frac{h + \sqrt{h^2 + 4n}}{n}\beta \quad (12)$$

By comparison of $\Delta\epsilon_{\pi}^{\text{O-Au}}$, $\Delta\epsilon_{\pi}^{\text{Au-O-Au}}$, and $\Delta\epsilon_{\pi}^{\text{O-(Au)}_n}$, it is found that $\Delta\epsilon_{\pi}^{\text{O-Au}}$ is lowest and $\Delta\epsilon_{\pi}^{\text{O-(Au)}_n}$ is highest. This indicates that the Au–O bond in O–Au is strongest among O–Au, Au–O–Au, and O–(Au)_n. $\Delta\epsilon_{\pi}$ is increased with the increase of the coordinate number of O, implying that every O–Au bond is weakened if O is connected with more Au atoms. Compared with $\Delta\epsilon_{\pi}^{\text{O-Au}}$, $\Delta\epsilon_{\pi}^{\text{O-Au-O}}$, and $\Delta\epsilon_{\pi}^{\text{Au-(O)}_n}$, it is found that $\Delta\epsilon_{\pi}^{\text{O-Au-O}}$ is the lowest. This indicates that the Au–O bond in O–Au–O is the strongest among O–Au, O–Au–O, and Au–(O)_n. It is also easy to prove that $\Delta\epsilon_{\pi}^{\text{O-Au-O}}$ is the lowest one among all the structures, which indicates that the bond of Au–O in O–Au–O is the strongest. This suggests that the atomic oxygen adsorption on gold surfaces prefers to form a linear O–Au–O structure. The present argument of the Au–O bond energy can be also generalized by the analysis of the Au–O bond order in the Au–O, Au–O–Au, and O–Au–O structures as given in detail in the Supporting Information with Figure 1S.

During the formation of Au–O bond, the contribution from a 6s electron of gold should also be considered. Since the antibonding orbital of the Au–O π -bond is not fully filled, the 6s electron of gold could transfer to this orbital as shown in Figure 3. If the 6s orbital level is significantly higher than the

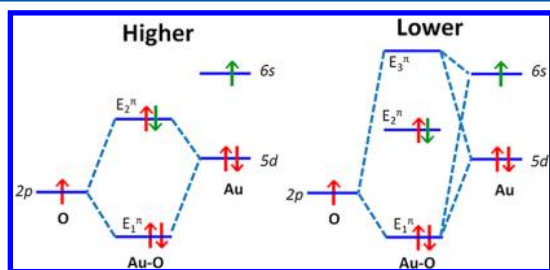





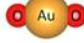


Figure 3. Schematic diagrams for energy gain of Au–O from a 6s electron. The left (right) diagram show the situation of 6s orbital higher (lower) than the π -antibonding level composed of 2p of O and 5d of Au. To clarify, the 6s electrons are marked as green color.

antibonding orbital of the Au–O π -bond, the transference of the 6s electron is direct to the antibonding orbital, as given in the left part of Figure 3. Otherwise, it will participate into the Au–O bond formation via a new nonbonding orbital, as shown in the right part of Figure 3. In any case, the system becomes more stable by the energy gain of the 6s electron transfer to the Au–O orbital. Similarly to Au–O, the structures of Au–O–Au, O–Au–O, O–(Au)_n, and Au–(O)_n become more stable by the contribution of the 6s electron transfer. To clarify, for Au–O–Au as an example, the molecular orbitals involving the distribution of a 6s electron are shown in Figure 2S, Supporting Information.

■ EXAMINATION BY DFT CALCULATIONS

To prove the Au–O bond in O–Au–O is stronger than the others, the bond length and bond energy of Au–O in several cluster models are obtained by DFT calculations as listed in Table 1. Comparing with O–Au, Au–O–Au, and O–(Au)₃, it

Table 1. Bond Length and Bond Energy of Au–O in Simple Cluster Models

	Bond length of Au–O (Å)	Total binding energy (eV)	Bond energy of Au–O (eV)
	1.873	2.93	2.93
	1.962	4.10	2.05
	1.965	5.18	2.59
	1.800	6.92	3.46
	1.815	9.05	3.02
	2.037	6.09	2.03

is found that the total binding energy is increased from 2.93 to 6.09 eV when the coordinate number for oxygen increases from one to three, whereas the bond energy of every Au–O is decreased from 2.93 to 2.03 eV at the same time. The sequence of the total binding energies for the Au–O, Au–O–Au, and O–(Au)₃ clusters agrees well with the sequence of the π -bond energies (eqs 3, 4, and 6) from Hückel theory. This also implies that the adsorption sites for the oxygen atom on a Au surface favors the multifold sites over the top sites.

Comparing with O–Au, O–Au–O, and Au–(O)₃, it is found that the total binding energy increased from 2.93 to 9.05 eV gradually. The average Au–O bond energy in the linear O–Au–O structure is 3.46 eV, which is stronger than those in the Au–O and O–(Au)₃ with the bond energies of 2.93 and 3.02 eV. The sequences of the total binding energy and the average Au–O bond energy are in good agreements with the prediction from Hückel theory. The Au–O bond length in the linear O–Au–O structure is 1.800 Å, which is shorter than those in the Au–O, two Au–O–Au, Au–(O)₃, and O–(Au)₃ clusters with the bond lengths of 1.873, 1.962, 1.965, 1.815, and 2.037 Å, respectively. The shortest bond length and the largest bond energy of Au–O bond in the linear O–Au–O structure also imply that the linear O–Au–O structure is the most stable, as predicted by Hückel theory.

To examine the validity of the prediction by Hückel theory in realistic surface models, the atomic oxygen adsorption on the flat Au(111), Au(100), and Au(110) surfaces and the stepped Au(211) and Au(321) surface is investigated. The structures with single atomic oxygen adsorption on Au surfaces are shown in Figure 4, and the corresponding adsorption energies are listed in Table 2. The adsorption energies for the top site on the Au(111), Au(100), Au(110), Au(211), and Au(321) surfaces are −2.06, −2.09, −2.35, −2.39, and −2.46 eV,

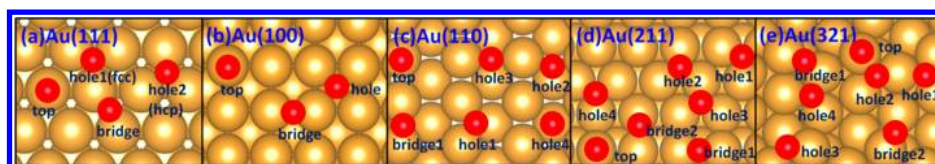


Figure 4. Adsorption sites for single atomic oxygen on the Au(111) (a), Au(100) (b), Au(110) (c), Au(211) (d), and Au(321) (e) surfaces. The golden and red balls denote the Au and O atoms, respectively.

Table 2. Single Atomic Oxygen Adsorption Energies (eV) on Gold Surfaces

site		Au(111)	Au(100)	Au(110)	Au(211)	Au(321)
top		−2.06	−2.09	−2.35	−2.39 ^a	−2.46
bridge	bridge1	−2.96 ^a	−3.21	−3.31	−3.45	−3.33
	bridge2				−2.98	−3.09
hole	hole1	−3.39	−3.24	−3.43	−3.48	−3.48
	hole2	−3.18		−3.00	−3.40	−3.35
	hole3			−2.99	−3.12	−3.27
	hole4			−2.83	−3.04	−3.27

^aUnstable structure.

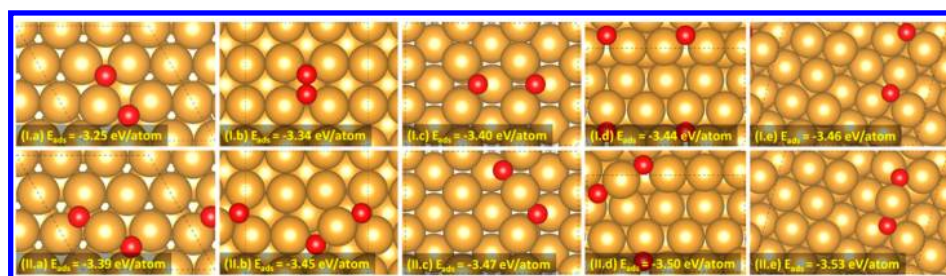


Figure 5. Adsorption structures and energies for two-oxygen adsorption on the Au(111) (a), Au(100) (b), Au(110) (c), Au(211) (d), and Au(321) (e) surfaces, respectively. (I) The most stable structures without formation of a linear O–Au–O structure. (II) The most stable structures with formation of a linear O–Au–O structure. The golden and red balls denote the Au and O atoms, respectively.

respectively, which are higher by 0.90–1.12 eV than those at the bridge sites. The adsorption energies for the most stable bridge sites on these surfaces are 0.03–0.43 eV higher than those for the most stable hole sites. This indicates that the oxygen atom prefers to locate at the multifold sites (hole sites), which agrees with the prediction from Hückel theory. The most stable sites for atomic oxygen adsorption are the hole sites in our work, which is in good agreement with the results reported by Fajin et al.¹⁷ However, it disagrees with the results of the bridge sites as the most stable site for oxygen adsorption on the Au(211) surface reported by Liu et al.¹⁹ The disagreement between Liu's results and ours may originate from different computational parameters since the energy difference between the bridge site and hole site is only 0.03 eV, which is in the range of DFT error. Note that the neighboring gold atoms can also affect the oxygen adsorption, just like it does to CO adsorption.²⁶ Therefore, we still believe that it is possible to find some gold surfaces with the bridge site as the most stable adsorption site.

From Hückel theory, we know that the adsorbed oxygen on Au surfaces prefers to form a linear O–Au–O structure. Thus, we investigate the two-oxygen adsorption on the Au(111), Au(100), Au(110), Au(211), and Au(321) surfaces. Similarly to the variety of single oxygen atom adsorption, there are also many different structures for the double oxygen adsorption. To clarify the situations, only the most stable structures with and without the formation of linear O–Au–O structures are displayed in Figure 5. The top row (series I) in Figure 5 shows the most stable two-oxygen adsorption structures without

formation of a linear O–Au–O structure, and the bottom row (series II) gives the most stable two-oxygen adsorption structures with a linear O–Au–O structure. The adsorption structures with linear O–Au–O structures (series II) are more stable by 0.12–0.28 eV than those without the linear O–Au–O structure (series I) on all the Au surfaces. This suggests that the formation of a linear O–Au–O structure is thermodynamically favorable on Au surfaces for atomic oxygen adsorption.

With the formation of the stable linear O–Au–O structure, the surprising first order kinetics of O₂ desorption from Au surfaces may be explained easily. Every two oxygen atoms on Au surfaces should be always coupling to form the linear O–Au–O structure, and the diffusion barrier of an oxygen atom from the O–Au–O structure should be very high because of the high stability of the O–Au–O structure. The O₂ desorption from Au surfaces should occur directly from the linear O–Au–O structure, and the atomic oxygen diffusion on the surface before desorption is not required. Therefore, the O₂ desorption from Au surfaces is observed as the first order kinetics. Furthermore, the calculated O₂ desorption barrier from the linear O–Au–O structure (Figure 5II.a) on the Au(111) surface is 1.68 eV, in reasonable agreement with the experimental values: 1.3,³² 1.43,²² and 1.47 eV.³³ This viewpoint based on the stable linear O–Au–O structure provides one possible explanation for the surprising first order kinetics behavior, and more theoretical or experimental evidence are needed throughout to understand this phenomenon.

■ CONCLUSIONS

Atomic oxygen adsorption on Au surfaces was investigated by the Hückel theory and DFT calculations. From Hückel theory, it is found that atomic oxygen prefers to locate at multifold sites (hole sites) on Au surfaces with the formation of a linear O–Au–O structure. The predictions are confirmed by DFT calculations in the cluster models and realistic surface slab models. The preference of linear O–Au–O structures for atomic oxygen on gold surfaces may well explain the peculiar O₂ desorption behavior observed in the TPD experiments. The linear O–Au–O structure as the most stable adsorption structure is quite different from the conventional view of single atomic oxygen adsorption and should lead to different interpretations for the reaction mechanism of low-temperature CO oxidation on nano gold catalysts.

■ ASSOCIATED CONTENT

Supporting Information

Analysis of the Au–O bond order in the Au–O, Au–O–Au, and O–Au–O structures and the molecular orbitals of Au–O–Au molecule. This material is available free of charge via the Internet at <http://pubs.acs.org>.

■ AUTHOR INFORMATION

Corresponding Author

*E-mail: keju.sun@aist.go.jp.

Author Contributions

The manuscript was written through contributions of all authors. All authors have given approval to the final version of the manuscript.

Notes

The authors declare no competing financial interest.

■ ACKNOWLEDGMENTS

This study was supported by a Grant-in-Aid for Specially Promoted Research, grant 19001005, from the Ministry of Education, Culture, Sports, Science and Technology, Japan.

■ REFERENCES

- (1) Haruta, M.; Kobayashi, T.; Sano, H.; Yamada, N. *Chem. Lett.* **1987**, *16*, 405–408.
- (2) Valden, M.; Lai, X.; Goodman, D. W. *Science* **1998**, *281*, 1647–1650.
- (3) Hashmi, A. S. K.; Hutchings, G. J. *Angew. Chem., Int. Ed.* **2006**, *45*, 7896–7936.
- (4) Mavrikakis, M.; Stoltze, P.; Norskov, J. K. *Catal. Lett.* **2000**, *64*, 101–106.
- (5) Hughes, M. D.; Xu, Y. J.; Jenkins, P.; McMorn, P.; Landon, P.; Enache, D. I.; Carley, A. F.; Attard, G. A.; Hutchings, G. J.; King, F.; et al. *Nature* **2005**, *437*, 1132–1135.
- (6) Enache, D. I.; Edwards, J. K.; Landon, P.; Solsona-Espriu, B.; Carley, A. F.; Herzing, A. A.; Watanabe, M.; Kiely, C. J.; Knight, D. W.; Hutchings, G. J. *Science* **2006**, *311*, 362–365.
- (7) Bravo-Suarez, J. J.; Bando, K. K.; Lu, J. L.; Haruta, M.; Fujitani, T.; Oyama, S. T. *J. Phys. Chem. C* **2008**, *112*, 1115–1123.
- (8) Haruta, M. *Catal. Today* **1997**, *36*, 153–166.
- (9) Schubert, M. M.; Hackenberg, S.; van Veen, A. C.; Muhler, M.; Plzak, V.; Behm, R. J. *J. Catal.* **2001**, *197*, 113–122.
- (10) Costello, C. K.; Kung, M. C.; Oh, H. S.; Wang, Y.; Kung, H. H. *Appl. Catal., A* **2002**, *232*, 159–168.
- (11) Liu, Z. P.; Gong, X. Q.; Kohanoff, J.; Sanchez, C.; Hu, P. *Phys. Rev. Lett.* **2003**, *91*, 266102.
- (12) Remediakis, I. N.; Lopez, N.; Norskov, J. K. *Angew. Chem., Int. Ed.* **2005**, *44*, 1824–1826.
- (13) Sinha, A. K.; Seelan, S.; Tsubota, S.; Haruta, M. *Top. Catal.* **2004**, *29*, 95–102.
- (14) Molina, L. M.; Hammer, B. *Appl. Catal., A* **2005**, *291*, 21–31.
- (15) Akita, T.; Tanaka, K.; Kohyama, M. *J. Mater. Sci.* **2008**, *43*, 3917–3922.
- (16) Fajin, J. L. C.; Cordeiro, M. N. D. S.; Gomes, J. R. B. *J. Phys. Chem. C* **2008**, *112*, 17291–17302.
- (17) Fajin, J. L. C.; Cordeiro, M. N. D. S.; Gomes, J. R. B. *J. Phys. Chem. C* **2007**, *111*, 17311–17321.
- (18) Fajin, J. L. C.; Cordeiro, M. N. D. S.; Gomes, J. R. B. *Surf. Sci.* **2008**, *602*, 424–435.
- (19) Liu, Z. P.; Hu, P.; Alavi, A. *J. Am. Chem. Soc.* **2002**, *124*, 14770–14779.
- (20) Parker, D. H.; Koel, B. E. *J. Vac. Sci. Technol., A* **1990**, *8*, 2585–2590.
- (21) Sault, A. G.; Madix, R. J.; Campbell, C. T. *Surf. Sci.* **1986**, *169*, 347–356.
- (22) Deng, X. Y.; Min, B. K.; Guloy, A.; Friend, C. M. *J. Am. Chem. Soc.* **2005**, *127*, 9267–9270.
- (23) Gottfried, J. M.; Schmidt, K. J.; Schroeder, S. L. M.; Christmann, K. *Surf. Sci.* **2002**, *511*, 65–82.
- (24) Hückel, E. *Z. Angew. Phys.* **1931**, *70*, 204–286.
- (25) Hoffmann, R. *J. Chem. Phys.* **1963**, *39*, 1397–1412.
- (26) Sun, K. J.; Kohyama, M.; Tanaka, S.; Takeda, S. *J. Comput. Chem.* **2011**, *32*, 3276–3282.
- (27) Kresse, G.; Hafner, J. *Phys. Rev. B* **1993**, *48*, 13115–13118.
- (28) Perdew, J. P.; Burke, K.; Ernzerhof, M. *Phys. Rev. Lett.* **1996**, *77*, 3865–3868.
- (29) Blochl, P. E. *Phys. Rev. B* **1994**, *50*, 17953–17979.
- (30) Kresse, G.; Joubert, D. *Phys. Rev. B* **1999**, *59*, 1758–1775.
- (31) Sun, K. J.; Zhao, Y. H.; Su, H. Y.; Li, W. X. *Theor. Chem. Acc.* **2012**, *131*, 1118.
- (32) Saliba, N.; Parker, D. H.; Koel, B. E. *Surf. Sci.* **1998**, *410*, 270–282.
- (33) Davis, K. A.; Goodman, D. W. *J. Phys. Chem. B* **2000**, *104*, 8557–8562.